

# Removal of cadmium from aqueous solution by organic-inorganic hybrid sorbent combining sol-gel processing and imprinting technique

Jin-Bao Wu\*\*\* and Yan-Li Yi\*\*†

\*Land and Environment College, Shenyang Agriculture University, Shenyang 110161, China

\*\*College of Applied Chemistry, Shenyang University of Chemical Technology, Shenyang 110142, China

(Received 20 August 2012 • accepted 23 December 2012)

**Abstract**—An organic-inorganic hybrid sorbent with high adsorption capacity was prepared by surface imprinting technique combined with sol-gel processing with 3-[2-(2-aminoethylamino)ethylamino]propyl-trimethoxysilane as a functional precursor and silica as the support for the removal of Cd(II) ion from aqueous solution, and was characterized by Fourier-transform infrared spectroscopy, scanning electron microscopy, nitrogen gas sorption and thermogravimetric analysis. The influences of different adsorption parameters, such as pH value of solution, contact time and the initial concentrations of Cd(II) ions on the adsorption amount of Cd(II), were examined. The optimum pH for adsorption was found to be in the range of 4-8. The adsorption rate of Cd(II) on the imprinted hybrid sorbent was rapid. The relative selectivity coefficients of the imprinted hybrid sorbent were higher than those of the non-imprinted sorbent. Ho's pseudo-second-order model best described the kinetics of the adsorption reaction. The adsorption process of metals followed Redlich-Peterson and Langmuir isotherms models, and the experimental value of maximum adsorption capacity for Cd(II) was 77.2 mg·g<sup>-1</sup>. The positive values of  $\Delta H^\circ$  suggested endothermic nature of Cd(II) adsorption on the imprinted hybrid sorbent. Increase in entropy of adsorption reaction was shown by the positive values of  $\Delta S^\circ$  and the negative values of  $\Delta G^\circ$  indicating that the adsorption was spontaneous.

Key words: Cadmium, Ion Imprinted, Sol-gel, Hybrid, Removal

## INTRODUCTION

Cadmium (Cd), a member of group IIb in the periodic table of elements, is widely used in various industrial processes: active electrode materials in nickel-cadmium batteries, pigments used mainly in plastics, engineering coatings on steel and some nonferrous metals, components of various specialized alloys and so on [1,2]. It is also one of the most toxic heavy metals because of its toxicity to humans through eating food, drinking water, breathing or smoking. It has been classified as a human carcinogen by the International Agency for Research on Cancer [1,2].

Several physical and chemical methods, including precipitation, membrane separation technique, ion exchange technique and solvent extraction technique, have been used to remove Cd(II) from aqueous solution [3]. One of the most promising alternative methods for heavy metal removal is the adsorption of pollutant ions on functionalized materials. There are many types of sorbents, including activated carbon [4], oxide minerals [5,6], resins [7,8], polymeric hybrid sorbents [9-11], functionalized silica gel [12,13], waste materials [14,15], and biosorbents [16,17], which have been used to adsorb metal ions or to enrich trace amounts of metals from aqueous solutions. Recently, ionic imprinted polymers (IIPs) have been attractive materials that enable the selective extraction, separation and removal of cadmium from complex mixtures [18-22]. The preparation of IIPs based on the ion-imprinting concept was described: a matrix is synthesized in the presence of an ionic template and chelat-

ing resins are then obtained by removal of the targeted ion [23,24]. The cavities thus obtained in the polymer exhibit high selectivity to wards specific metal ions. Ionic imprinted functionalized materials with outstanding advantages (such as being simple, convenient to prepare, high selectivity, fast mass transport rates, good mechanical and thermal stabilities) have been developed for the selective removal or separation of heavy metals from aqueous solution [23-26]. Recently, ionic imprinted functionalized hybrid sorbent prepared by combining sol-gel processing and imprinting technique has shown high adsorption capacity, which determines how much sorbent is required to quantitatively concentrate the targeted ion from a given solution. However, the synthesis of ionic imprinted functionalized hybrid sorbent by combining sol-gel processing and imprinting method has been reported in only a few articles [27-29].

We synthesized a Cd(II) imprinted hybrid sorbent via combining sol-gel processing and imprinting method for the removal of cadmium(II) ion from aqueous solutions. The materials were characterized by scanning electron microscopy, nitrogen gas sorption, Fourier-transform infrared spectroscopy (FT-IR) and thermogravimetric analysis. Adsorption behaviors, adsorption isotherm, kinetics and thermodynamic of Cd(II) adsorption onto the imprinted hybrid sorbent were studied.

## EXPERIMENTAL

### 1. Materials

3-[2-(2-Aminoethylamino)ethylamino]propyl-trimethoxysilane (A<sub>3</sub>PTS) was obtained from Sigma. The tetraethoxysilane (TEOS), ethanol, CdCl<sub>2</sub>·2.5H<sub>2</sub>O, ZnCl<sub>2</sub>, CoCl<sub>2</sub>·6H<sub>2</sub>O, NiCl<sub>2</sub>·6H<sub>2</sub>O, CuCl<sub>2</sub>·2H<sub>2</sub>O,

†To whom correspondence should be addressed.  
E-mail: yilianli@126.com

Pb(NO<sub>3</sub>)<sub>2</sub>, NaOH, HCl and NH<sub>3</sub>·H<sub>2</sub>O were purchased from Sinopharm Chemical Reagent Co., Ltd. Shanghai, China.

## 2. Apparatus

FT-IR spectra (4,000–450 cm<sup>-1</sup>) with KBr pellets and a resolution of 1 cm<sup>-1</sup> were recorded using a Nicolet 6700 FT-IR spectrometer (Thermo Fisher Scientific Inc., USA). The surface morphology of the Cd(II)-imprinted hybrid sorbent was examined with scanning electron microscopy (SEM, Shimadzu Corporation, Japan) at the desired magnification. An ASAP-2010C surface analyzer (Micromeritics, USA) was used for the research of surface area. An AA-6300c flame atomic absorption spectrometer (FAAS, Shimadzu Corporation, Japan) was used to measure the concentrations of Cd(II), Cu(II), Co(II), Zn(II), Ni(II) and Pb(II) in aqueous solutions after appropriate dilutions and acidification to pH ~2 adjusted with HNO<sub>3</sub>. Thermogravimetric analysis was performed on a Beijing Scientific Instrument Factory HCT-2 thermogravimetric analyzer. The solution blanks were below the instrument detection limits of 15 µg L<sup>-1</sup> for Cd(II), 20 µg L<sup>-1</sup> for Cu(II), 20 µg L<sup>-1</sup> for Zn(II), 30 µg L<sup>-1</sup> for Co(II), 30 µg L<sup>-1</sup> for Ni(II) and 300 µg L<sup>-1</sup> for Pb(II). A PB-10 pH meter (Sartorius, German) was used for the pH adjustments.

## 3. Preparation and Characterization of Cd(II)-imprinted Hybrid Sorbent

The Cd(II)-imprinted hybrid sorbent was prepared by base-catalyzed sol-gel process with 0.1 mol L<sup>-1</sup> of ammonium hydroxide solution [27–29]. Solution (a) was prepared by mixing 20 mL of TEOS and 10 mL of H<sub>2</sub>O and the pH was adjusted at 2.0 with the addition of 1 M HCl for stirring 30 min. Solution (b) was prepared by mixing 1.92 g of CdCl<sub>2</sub>·2.5H<sub>2</sub>O which was dissolved in 40 mL of methanol and 40 mL of H<sub>2</sub>O and 4 mL of A<sub>3</sub>PTS under stirring for 1 h. Solutions (a) and (b) were mixed and added dropwise NH<sub>4</sub>OH 0.1 M (pH≈5) under stirring at 333 K for 30 min. Gel formed was aged for 48 h at room temperature. Then, the white solid was filtered and washed by 1 mol L<sup>-1</sup> HCl solution until the cadmium concentration in the washings was undetectable by FAAS. The resulting gels were neutralized with 0.1 mol L<sup>-1</sup> NaHCO<sub>3</sub> to pH 7.5, filtered, washed with deionized water, and dried under vacuum at 60 °C for 12 h. Furthermore, the Cd(II)-imprinted hybrid sorbent was sieved to obtain a particle size between 100 and 200 mesh. For comparison, the non-imprinted sorbent was also prepared using an identical procedure, but without the addition of CdCl<sub>2</sub>·2.5H<sub>2</sub>O.

The Cd(II)-imprinted hybrid sorbent was characterized by IR, SEM and thermogravimetric analysis spectra. The surface area was determined from adsorption-desorption isotherms of nitrogen at 77 K. Specific surface areas were estimated by using the BET equation.

## 4. Cadmium Adsorption Experiments

Adsorption of Cd(II) from aqueous solutions was investigated in batch experiments. For the effect of pH on the adsorption capacity, 100 mg of the Cd(II)-imprinted hybrid sorbent was introduced into 25 mL of 400 mg L<sup>-1</sup> Cd(II) solution in the pH range of pH 2–10. To measure the maximum adsorption capacity, 100 mg of Cd(II)-imprinted hybrid sorbent was equilibrated with 25 mL of the various concentration of Cd(II) solution (25–800 mg L<sup>-1</sup>) at pH 6. The adsorption kinetic of Cd(II)-imprinted hybrid sorbent was studied at pH 6 for different adsorption time (5–60 min). The suspensions were brought to the desired pH by adding sodium hydroxide and nitric acid. The selective adsorption experiments of Cu(II), Co(II), Pb(II), Ni(II) and Zn(II) ions with respect to Cd(II) ions were con-

ducted using Cd(II)-imprinted hybrid sorbent or non-imprinted sorbent. The Cd(II)-imprinted hybrid sorbent (100 mg) was added to 25 mL of binary metal mixed aqueous solution containing 50 mg·L<sup>-1</sup> Cd(II)/Cu(II), Cd(II)/Zn(II), Cd(II)/Co(II), Cd(II)/Ni(II) and Cd(II)/Pb(II) at a pH of 6 in the flasks with stirring. After adsorption equilibrium, the concentration of each ion in the remaining solution was measured by FAAS. The distribution and selectivity coefficients of Cu(II), Co(II), Pb(II), Ni(II) and Zn(II) with respect to Cd(II) can be obtained from equilibrium binding data according to Eqs. (1) and (2) [30].

$$K_d = [(C_i - C_f)/C_f](V/m) \quad (1)$$

In Eq. (1),  $K_d$  represents the distribution coefficient;  $C_i$  and  $C_f$  are the initial and final concentrations of metal ions (mg L<sup>-1</sup>), respectively.  $V$  is the volume of the solution (mL);  $m$  is the mass of the imprinted sorbent used (g).

$$k = K_d(\text{Cd(II)})/K_d(\text{X(II)}) \quad (2)$$

In Eq. (2),  $k$  is the selectivity coefficient, and X(II) represents Cu(II), Co(II), Pb(II), Ni(II) and Zn(II) ions. A comparison of the  $k$  values of Cd(II)-imprinted hybrid sorbent or the non-imprinted sorbent with those metal ions allows an estimation of the effect of imprinting on selectivity.

A relative selectivity coefficient  $k'$  (Eq. (3)) can be defined as

$$k' = k_{\text{imprinted}}/k_{\text{non-imprinted}} \quad (3)$$

Results from the comparison of the  $k'$  values of Cd(II)-imprinted hybrid sorbent with non-imprinted sorbent allow an estimation of the effect of imprinting on selectivity.

To obtain the reusability of the Cd(II)-imprinted hybrid sorbent, adsorption-desorption cycle was repeated nine by times using the same sorbent. Adsorbed metal ions were desorbed by treatment with 50 mL of 3 mol L<sup>-1</sup> HCl solution at room temperature stirring at 400 rpm for 2 h [30]. The sorbents were washed again with deionized water and dried under vacuum at 60 °C overnight before another extraction cycle.

For all sample determinations, a triplicate run was considered and the samples were analyzed in replicates of three as well. For each set of data present, standard statistical methods were used to determine the mean values and standard deviations. Confidence intervals of 95% were calculated for each set of samples to determine the margin of error.

## 5. The Adsorption Isotherms

To investigate the adsorption isotherms, three equilibrium models, Langmuir, Freundlich equations and Redlich-Peterson isotherm, were applied. The Langmuir isotherm [31] is often used to describe adsorption of a solute from a liquid solution. The linear representation of this model for single-component adsorption is:

$$C_{eq}/q_{eq} = 1/(q_{max} b) + C_{eq}/q_{max} \quad (4)$$

where  $q_{eq}$  is the amount of adsorbed metals in the sorbent (mg g<sup>-1</sup>),  $C_{eq}$  is the equilibrium ion concentration in solution (mg L<sup>-1</sup>),  $b$  (L mg<sup>-1</sup>) is the equilibrium constant related to the adsorption energy, and  $q_{max}$  is the maximum adsorption capacity (mg g<sup>-1</sup>).

The Freundlich isotherm [32] provides an empirical relationship between the adsorption capacity and the equilibrium concentration of the sorbent. Linear form of this model is:

$$\ln q_{eq} = \ln K_F + (1/n) \ln C_{eq} \quad (5)$$

where  $K_F$  and  $n$  are the Freundlich parameters that are related to the adsorption capacity and adsorption intensity, respectively.

Redlich-Peterson isotherm is a hybrid isotherm featuring both Langmuir and Freundlich isotherms [33], which incorporates three parameters into an empirical equation and can be applied either in homogeneous or heterogeneous systems due to its versatility [34]. It approaches the Freundlich isotherm model at high concentration (as the exponent  $g$  tends to zero) and is in accordance with the low concentration limit of the ideal Langmuir condition (as the  $g$  value is close to one) [34]. It can be represented in a linear expression as Eq. (6):

$$\frac{C_{eq}}{q_{eq}} = \frac{1}{K_R} + \frac{a_R}{K_R} C_{eq}^g \quad (6)$$

where,  $K_R$  Redlich-Peterson isotherm constant ( $L g^{-1}$ );  $a_R$  Redlich-Peterson isotherm constant ( $L mg^{-1}$ );  $g$  Redlich-Peterson isotherm exponent which lies between 0 and 1—it has two limiting behaviors: Langmuir form for  $g=1$  and Henry's law form for  $g=0$ .

Plotting the left-hand side of Eq. (6) against  $C_{eq}^g$  to obtain the isotherm constants is not applicable because of the three unknowns,  $a_R$ ,  $K_R$  and  $g$ . Therefore, a minimization procedure is adopted to solve Eq. (6) by maximizing the correlation coefficient between the theoretical data for  $q_{eq}$  predicted from Eq. (6) and experimental data.

## 6. Adsorption Kinetics

Adsorption kinetics is important in that it controls the efficiency of the process and the models correlate the adsorbate uptake rate with its bulk concentration. Experiments were also performed to understand the kinetics of Cd(II) adsorption by Cd(II)-imprinted hybrid sorbent. To analyze the adsorption rate, the kinetic data were modeled by pseudo-first-order [35], pseudo-second-order [36], Elovich model [37] and intraparticle diffusion models [38].

The linear form of pseudo-first-order model can be expressed as:

$$\log(q_e - q_t) = \log q_e - k_1 t / 2.303 \quad (7)$$

where  $k_1$  ( $min^{-1}$ ) is the rate constant of the pseudo-first adsorption.  $q_e$  and  $q_t$  ( $mg g^{-1}$ ) are the adsorption capacities at equilibrium and at time  $t$  (min), respectively. The rate constants  $k_1$ ,  $q_e$  and correlation coefficients  $r^2$  were calculated using the slope and intercept of plots of  $\lg(q_e - q_t)$  versus  $t$ .

The pseudo-second-order rate expression, which has been applied for analyzing chemisorption kinetics from liquid solutions, is linearly expressed as:

$$t/q_t = 1/k_2 q_e^2 + t/q_e \quad (8)$$

where  $k_2$  ( $g mg^{-1} min^{-1}$ ) is the rate constant of the pseudo-second-order adsorption. The rate constants  $k_2$ ,  $q_e$  and correlation coefficients  $r^2$  were calculated from the linear plots of  $t/q_t$  versus  $t$ .

The Elovich equation is another rate equation in which the absorbing surface is heterogeneous:

$$\frac{dq_t}{dt} = \alpha \exp(-\beta q_t) \quad (9)$$

Where  $\alpha$  is the initial adsorption rate ( $mg g^{-1} min^{-1}$ ), and  $\beta$  is the desorption constant ( $g mg^{-1}$ ) during any one experiment. Integrating this equation for the boundary conditions, Eq. (11) becomes

$$q_t = 1/\beta \ln(\alpha\beta) + 1/\beta \ln t \quad (10)$$

A plot of  $q_t$  vs.  $\ln t$  gives a linear trace with a slope of  $(1/\beta)$  and an intercept of  $1/\beta \ln(\alpha\beta)$ .

The intraparticle diffusion model is expressed as

$$q_t = k_i t^{0.5} \quad (11)$$

Where,  $k_i$  is the intraparticle diffusion rate constant ( $mg g^{-1} min^{-0.5}$ ) and is calculated by the slope of straight-line portion of plotting  $q_t$  vs.  $t^{0.5}$ .

## 7. Thermodynamic Studies

The free energy change ( $\Delta G^\circ$ ), enthalpy change ( $\Delta H^\circ$ ) and entropy change ( $\Delta S^\circ$ ) were evaluated using the following equations [39]:

$$K_0 = C_{Ae}/C_e \quad (12)$$

$$\Delta G^\circ = -RT \ln K_0 \quad (13)$$

$$\Delta G^\circ = \Delta H^\circ - T\Delta S^\circ \quad (14)$$

where  $K_0$  is the equilibrium constant,  $C_{Ae}$  and  $C_e$  (both in  $\mu mol L^{-1}$ ) are the equilibrium concentrations for solute on the sorbent and in the solution, respectively.  $R$  is the universal gas constant ( $8.314 J K^{-1} mol^{-1}$ ) and  $T$  (K) is temperature.

## RESULTS AND DISCUSSION

### 1. Characterization

FT-IR spectra of Cd(II)-imprinted hybrid sorbent are shown in Fig. 1. The presence of  $NH_2$  groups is reflected by vibration band at  $3,504 cm^{-1}$  and  $1,525 cm^{-1}$ . The absorption bands at  $2,872 cm^{-1}$  and  $2,820 cm^{-1}$  are assigned to vibrations of  $CH_2$  groups. The presence of OH groups is reflected by vibration band at  $3,328 cm^{-1}$  and  $1,635 cm^{-1}$  due to the surface silanol groups with hydrogen bond and the remaining adsorbed water molecules. A broad peak is noted at  $1,095 cm^{-1}$ , due to the siloxane vibrations of  $(SiO)_n$ . The broad peak has been shifted to lower wave numbers at  $1,055 cm^{-1}$ , while the shoulder is more clearly observed at  $1,181 cm^{-1}$  due to the vibration of  $\delta(Si-CH_2)$ . The band at  $974 cm^{-1}$  is assigned to Si-OH stretching. The bands at  $789 cm^{-1}$  and  $465 cm^{-1}$  are assigned to Si-O-Si stretching and Si-O-Si bending, respectively. These results suggest that  $A_3PTS$  has been successfully grafted onto the surface of silica after modification. Similar results had been observed by previous

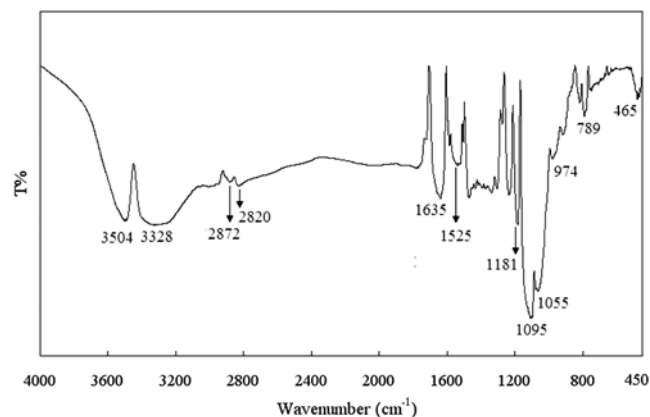
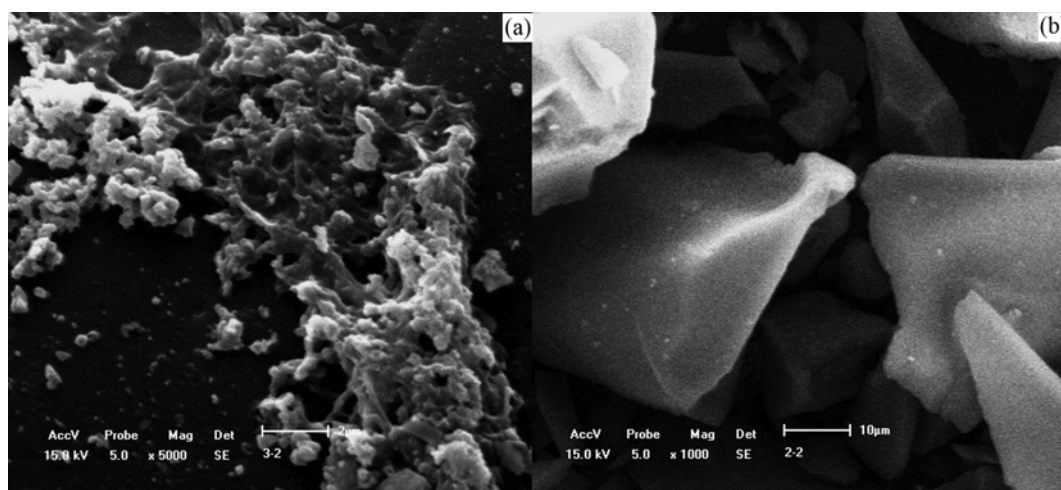


Fig. 1. IR spectra of Cd(II)-imprinted hybrid sorbent.



**Fig. 2.** SEM of Cd(II)-imprinted hybrid (a) sorbents and non-imprinted (b) sorbents.

studies [40,41].

The SEM images of Cd(II)-imprinted hybrid sorbent and non-imprinted sorbent were exemplified by the electron micrographs. As seen in Fig. 2, the surface morphology of Cd(II)-imprinted hybrid sorbent and non-imprinted sorbent is different. There are obviously some holes existing within the Cd(II)-imprinted hybrid sorbent. The results strongly show that the template imprint of Cd(II) was formed within Cd(II)-imprinted hybrid sorbent. Regarding the difference between the Cd(II)-imprinted hybrid sorbent and non-imprinted sorbent, it is important to mention the general role Cd(II) ion played in the preparation process of Cd(II)-imprinted hybrid sorbent. Assembled with Cd(II) as the pivot, monomers were regularly positioned around the templates by a coordinating bridge. Since the coordination bond was stronger than the hydrogen bond used in Cd(II)-imprinted hybrid sorbent, the relative motion of monomer-template was largely restricted. After polymerization and removed template, the imprint with a relative higher fidelity was thus left behind. The rough surfaces and smaller particle size of Cd(II)-imprinted sorbent should be considered a factor providing an increase in the surface area. The high surface area can reduce diffusion resistance and facilitate mass transfer. The specific surface area of the Cd(II)-imprinted hybrid sorbent and non-imprinted sorbent was found to be 152 and

101 m<sup>2</sup> g<sup>-1</sup>, respectively.

The DTA-TGA curves of Cd(II)-imprinted hybrid sorbent are shown in Fig. 3. DTA curves show the presence of three exothermic peaks at 256 °C, 325 °C and 495 °C attributed to the oxidative decomposition or combustion of the -NH<sub>2</sub>, -CH<sub>2</sub>-CH<sub>2</sub>- and C<sub>2</sub>H<sub>5</sub>O-groups. TGA curves exhibit an initial dried weight loss of 9% starting at 50 °C and ending at 200 °C due to a loss of residual water. Major decomposition occurs within the 200-600 °C interval with a weight loss of 27% which corresponds to the decomposition of the organic groups covalently bonded on the silica surface, together with the condensation of the remaining silanol groups to produce siloxane groups. A continuous and small weight loss (2%) is observed above 600 °C, which could be attributed to the combustion of residual organic material and/or to the desorption of water resulting from silanol condensation.

## 2. Effects of pH

The pH of the Cd(II) solution plays an important role in the whole adsorption process, particularly on the adsorption capacity. As shown

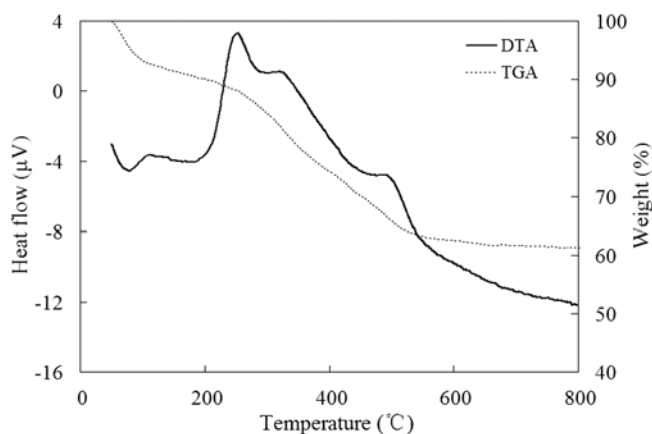


**Fig. 3.** TGA-DTA of Cd(II)-imprinted hybrid sorbent.

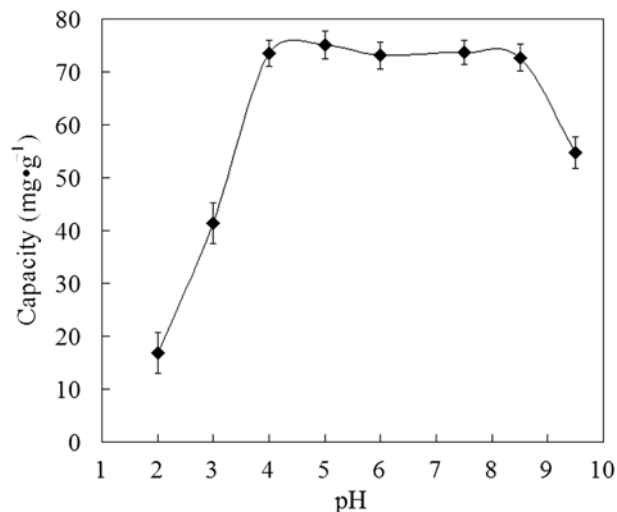


**Fig. 4.** Effect of initial solution pH on the adsorption capacity of Cd(II) onto Cd(II)-imprinted hybrid sorbent: Concentration of Cd(II)=400 mg·L<sup>-1</sup>, time=30 min, temperature=25 °C.

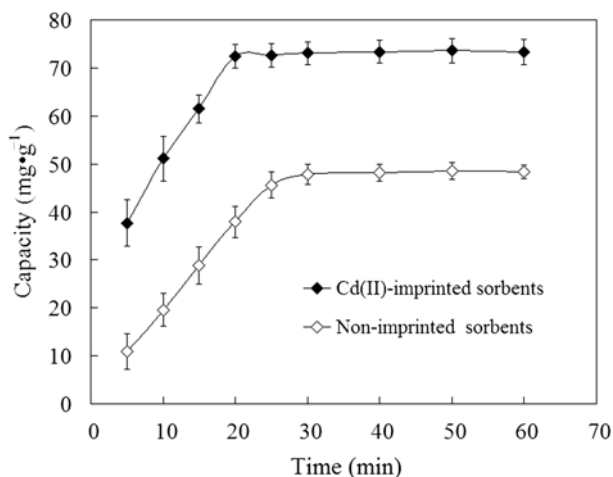


**Fig. 5.** Effect of the contact time on the adsorption capacity of Cd(II) onto Cd(II)-imprinted hybrid sorbent (◆) and non-imprinted sorbents (◇). Concentration of metals = 400 mg·L<sup>-1</sup>, pH = 6, temperature = 25 °C.

in Fig. 4, a consistent increase in adsorption capacity of Cd(II) is noticed as the pH is increased from 2-4, whereas pH in the range of 4-8, the adsorption capacity is only slightly affected by pH values. The lower adsorption capacity of Cd(II) at acidic pH might be due to the presence of excess H<sup>+</sup> ions competing with Cd(II) ions for the available adsorption sites. Small amount of metals is bound at pH > 8 due to the formation of insoluble hydroxide forms of metals. The optimum pH for metals uptake was recorded at pH range of 4-8.

### 3. Effect of Contact Time

The adsorption processes as a function of time to determine the point of equilibrium were studied from the adsorption experiments of Cd(II) ions onto Cd(II)-imprinted hybrid sorbent. The results are shown in Fig. 5, compared with the imprinted polymers which were prepared by polymerization method, where it was clear that adsorption of Cd(II) ions into Cd(II)-imprinted hybrid sorbent was rather quick and after 20 min the complete adsorption equilibrium between the two phases was obtained. This fast adsorption equilibrium was most probably due to high complexation and geometric shape affinity (or memory) between Cd(II) ions and the cavities of Cd(II) ions in the structure of Cd(II)-imprinted hybrid sorbent.

### 4. Effects of the Initial Metal Concentrations

Fig. 6 shows the initial concentration of Cd(II) ion dependence of the adsorbed amount of the Cd(II) ions onto the Cd(II)-imprinted hybrid sorbent. The adsorption capacities increase with increasing the concentration of Cd(II) ions, and a saturation value is achieved at ion concentration of 400 mg L<sup>-1</sup>, which represents saturation of the active binding cavities on the Cd(II)-imprinted hybrid sorbent.

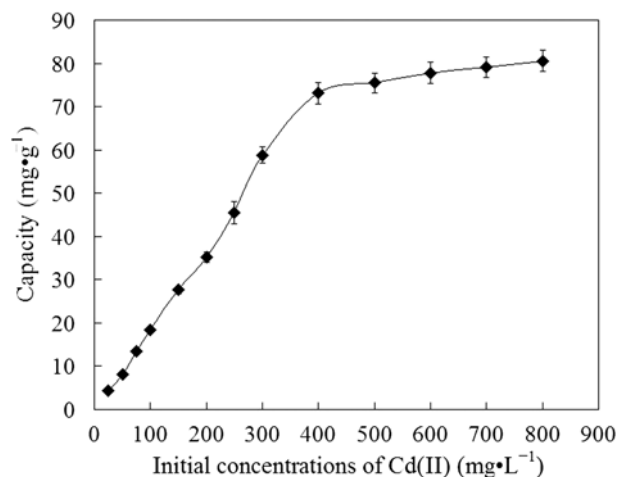


**Fig. 6.** Effect of initial concentration of solution on the adsorption amount of Cd(II) onto Cd(II)-imprinted hybrid sorbent: pH = 6, time = 30 min, temperature = 25 °C.

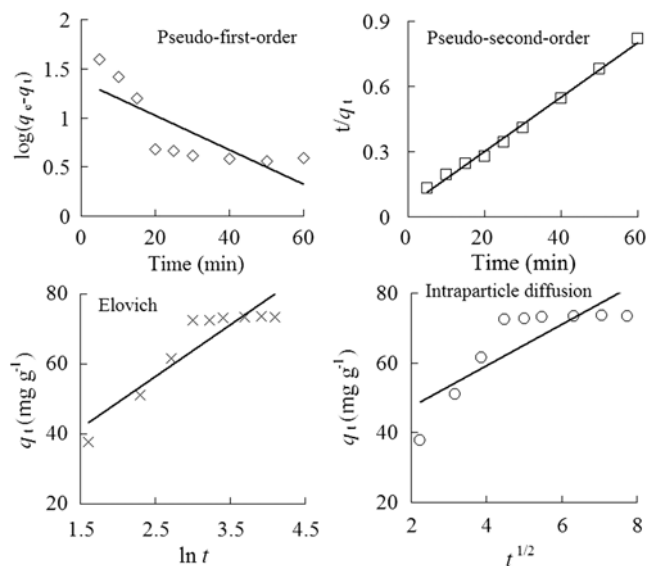


**Fig. 7.** The plots of pseudo-first-order (◇), pseudo-second-order (□), Elovich (×) and intraparticle diffusion (○) models for the adsorption of Cd(II) onto Cd(II)-imprinted hybrid sorbent.

The experimental value of adsorption capacity was 77.2 mg g<sup>-1</sup>.

### 5. Adsorption Dynamics

The linear pseudo-first-order, pseudo-second-order, Elovich model and intraparticle diffusion model plots for the adsorption of Cd(II) onto Cd(II)-imprinted hybrid sorbent were obtained by plotting lg(q<sub>∞</sub> - q<sub>t</sub>) vs. t, t/q<sub>t</sub> vs. t, q<sub>t</sub> vs. ln t and q<sub>t</sub> vs. t<sup>0.5</sup>, respectively (Fig. 7). The

**Table 1.** Calculated kinetic parameters for the adsorption of Cd(II) onto Cd(II)-imprinted hybrid sorbent

| Pseudo-first-order model                          | Pseudo-second-order model  | Elovich model                                      | Intraparticle diffusion model                                  |
|---|--|--|--|
| k <sub>1</sub> = 0.041 min <sup>-1</sup>          | k <sub>2</sub> = 3.02 × 10 <sup>3</sup> · mg <sup>-1</sup> · min <sup>-1</sup> | α = 54.97 mg · g <sup>-1</sup> · min <sup>-1</sup> | k <sub>i</sub> = 5.94 mg · g <sup>-1</sup> · min <sup>-1</sup> |
| q <sub>eq</sub> (cal) = 23.8 mg · g <sup>-1</sup> | q <sub>eq</sub> (cal) = 80 mg · g <sup>-1</sup>                                | β = 0.0675 g <sup>-1</sup> · mg                    |  |
| r <sup>2</sup> = 0.6393                           | r <sup>2</sup> = 0.9945  | r <sup>2</sup> = 0.8387                            | r <sup>2</sup> = 0.6928  |

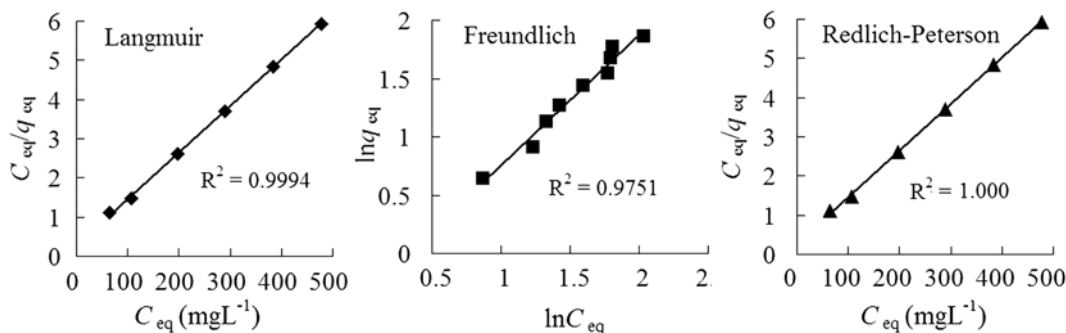


Fig. 8. The plots of Langmuir (◆), Freundlich (■) and Redlich-Peterson (▲) isotherms for the adsorption of Cd(II) onto Cd(II)-imprinted hybrid sorbent.

Table 2. Isotherms parameters for the adsorption of Cd(II) onto Cd(II)-imprinted hybrid sorbent

| Langmuir isotherm                            | Freundlich isotherm | Redlich-Peterson isotherm                 |
|--|---------------------|---|
| $q_{max}=84.03 \text{ mg}\cdot\text{g}^{-1}$ | $K_F=0.694$         | $K_R=3.663 \text{ L}\cdot\text{g}^{-1}$   |
| $b=0.044 \text{ L}\cdot\text{mg}^{-1}$       | $n=0.893$           | $a_R=0.0435 \text{ L}\cdot\text{mg}^{-1}$ |
|  |                     | $g=1$                                     |
| $R^2=0.9994$                                 | $R^2=0.9751$        | $R^2=1.000$                               |

kinetic parameters of Cd(II) are given in Table 1. The pseudo-second-order model well represents the experimental data ( $R^2>0.99$ ). The value of  $q_e$  (cal) of Cd(II)-imprinted hybrid sorbent was  $80 \text{ mg g}^{-1}$ . The theoretical  $q_e$  (cal) value estimated from the pseudo-second-order kinetic model was very close to the experimental value of  $q_e$  ( $77.2 \text{ mg g}^{-1}$ ). These results show that this sorbent system is well described by pseudo-second-order mechanism and chemisorption might be the rate-limiting step that controls the adsorption process.

## 6. Adsorption Isotherm

The relative parameters of Langmuir, Freundlich, and Redlich-Peterson isotherms by linear regression analysis were obtained from the plots of  $C_{eq}/q_{eq}$  vs.  $C_{eq}$ ,  $\ln q_{eq}$  vs.  $\ln C_{eq}$ , and  $C_{eq}/q_{eq}$  vs.  $C_{eq}^g$ , respectively (Fig. 8). In the case of Redlich-Peterson, the constants  $K_R$  were obtained by maximizing the  $r^2$  value using a trial and error method. The isotherm parameters are presented in Table 2.

The applicability of the isotherm equation to describe the adsorption process was judged by the correlation coefficients of isotherms ( $r^2$ ). The adsorption isotherm models fitted the data, based on the  $r^2$  values for the linear fitting, in the order of: Redlich-Peterson > Langmuir > Freundlich isotherm. The above order revealed that the equilibrium data were better fitted by the three-parameter models rather than the two-parameter models. In all cases, for Redlich-Peterson the isotherm exhibited the highest correlation coefficients, which produced a considerably better fit compared with the Langmuir and Freundlich isotherms. It could be also seen that the  $g$  values of Redlich-Peterson isotherm were 1, which means that the isotherm was the Langmuir but not the Freundlich isotherm. The theoretical  $q_{max}$  values ( $84.03 \text{ mg g}^{-1}$ ) of Cd(II) derived from Eq. (4) agreed very well with their experimental values ( $77.2 \text{ mg g}^{-1}$ ) in the case of Langmuir model. The result showed that the Redlich-Peterson and Langmuir isotherms had best-fit the equilibrium data for the adsorption behavior of Cd(II) on Cd(II)-imprinted hybrid sorbent, and the adsorption system was more likely monolayer coverage of the Cd(II)-im-

Table 3. The selectivity parameters of Cd(II)-imprinted hybrid sorbent for Cd(II)

| Metals        | Sorbents | $K_d$      |           | $k$   | $k'$ |
|---------------|----------|------------|-----------|-------|------|
|               |          | $K_d$ (Cd) | $K_d$ (X) |       |      |
| Cd(II)/Co(II) | IIP      | 9375       | 2068      | 4.53  | 33.8 |
|               | NIP      | 976        | 7268      | 0.134 |      |
| Cd(II)/Cu(II) | IIP      | 9484       | 2996      | 3.17  | 9.4  |
|               | NIP      | 2114       | 6236      | 0.339 |      |
| Cd(II)/Pb(II) | IIP      | 9864       | 1842      | 5.36  | 8.5  |
|               | NIP      | 3064       | 4852      | 0.631 |      |
| Cd(II)/Zn(II) | IIP      | 9342       | 2864      | 3.26  | 6.4  |
|               | NIP      | 3018       | 5904      | 0.511 |      |
| Cd(II)/Ni(II) | IIP      | 9865       | 2636      | 3.74  | 13.3 |
|               | NIP      | 1368       | 4864      | 0.281 |      |

printed hybrid sorbent surface by the Cd(II) ions.

## 7. Selectivity Experiment

Competitive adsorptions of Cd(II)/Cu(II), Cd(II)/Zn(II), Cd(II)/Ni(II), Cd(II)/Co(II) and Cd(II)/Pb(II) from their mixtures were also studied in a batch system. The Cu(II), Zn(II), Ni(II), Co(II) and Pb(II) ions were chosen as the competitor species because it has the same charge and also binds well with the amino groups. Table 3 summarizes  $K_d$ ,  $k$  and  $k'$  values of Cu(II), Zn(II), Ni(II), Co(II) and Pb(II) with respect to Cd(II).

A comparison of the  $K_d$  values for the Cd(II)-imprinted sorbent with the control (i.e., the non-imprinted sorbent) samples showed an increase in  $K_d$  for Cd(II), while  $K_d$  decreased for Cu(II), Zn(II), Ni(II), Co(II) and Pb(II).  $k'$  was an indicator to express metal adsorption affinity of recognition sites to the imprinted Cd(II) ions. These results showed that the  $k'$  values of the Cd(II)-imprinted sorbent for Cd(II)/Cu(II), Cd(II)/Zn(II), Cd(II)/Ni(II), Cd(II)/Co(II) and Cd(II)/Pb(II) were 9.4, 6.4, 13.3, 33.8 and 8.5 times greater than for the non-imprinted sorbent, respectively. The above facts suggest that the binding ability of the Cd(II)-imprinted sorbent for Cd(II) was far stronger than that for Cu(II), Zn(II), Ni(II), Co(II) and Pb(II). This was because the cavities imprinted by Cd(II) were not suited to Cu(II), Zn(II), Ni(II), Co(II) and Pb(II) in size, shape and spatial arrangement of action sites, resulting in high recognition ability and high selectivity of Cd(II)-imprinted for Cd(II). However, in the non-imprinted sorbent, the functional ligand arranged randomly and disorderly resulted in unremarkable selectivity performance.

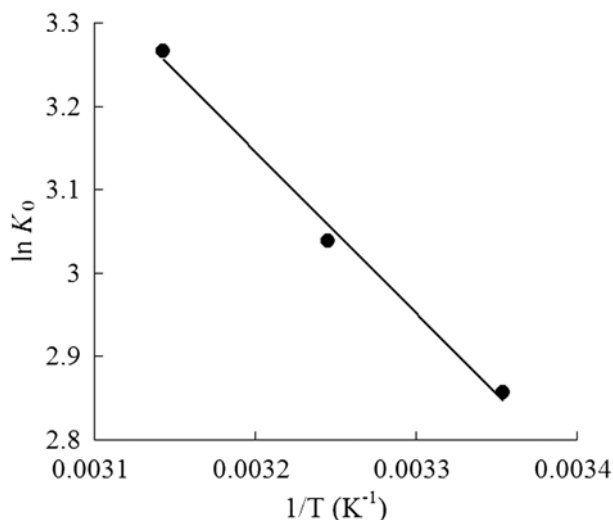


Fig. 9. Variation of equilibrium constant ( $K_0$ ) as a function of temperature ( $1/T$ ).

Table 4. Values of various thermodynamic parameters for adsorption of Cd(II) on Cd(II)-imprinted hybrid sorbent

| Thermodynamic constants                                 | Temperature (K) |        |        |
|---|-----------------|--------|--------|
|   | 298.15          | 308.15 | 318.15 |
| $\Delta G^\circ$ (kJ mol <sup>-1</sup> )                | -7.08           | -7.79  | -8.64  |
| $\Delta H^\circ$ (kJ mol <sup>-1</sup> )                | 16.09           | 16.09  | 16.09  |
| $\Delta S^\circ$ (J mol <sup>-1</sup> K <sup>-1</sup> ) | 77.64           | 77.64  | 77.64  |

### 8. Thermodynamic Parameters

Based on Eqs. (13) and (14), enthalpy change,  $\Delta H^\circ$  (kJ·mol<sup>-1</sup>), and entropy change,  $\Delta S^\circ$  (J·mol<sup>-1</sup>·K<sup>-1</sup>) were calculated from the slope and intercept of linear plot of  $\ln K_0$  versus  $1/T$ , respectively (as shown in Fig. 9). The thermodynamic parameters,  $\Delta G^\circ$ ,  $\Delta H^\circ$  and  $\Delta S^\circ$ , are shown in Table 4.  $\Delta H^\circ$  and  $\Delta S^\circ$  for the adsorption process were calculated to be 16.09 kJ mol<sup>-1</sup> and 77.64 J mol<sup>-1</sup> K<sup>-1</sup>, respectively. The negative value of  $\Delta G^\circ$  confirms the feasibility of the process and the spontaneous nature of adsorption with a high preference for Cd(II) onto Cd(II)-imprinted hybrid sorbent. The value of  $\Delta H^\circ$  was positive, indicating that the adsorption reaction was endothermic. The positive value of  $\Delta S^\circ$  showed the increasing randomness at the solid/liquid interface during the adsorption of Cd(II) ions onto Cd(II)-imprinted hybrid sorbent.

### 9. Regeneration

Regeneration of any exhausted sorbent is an important factor in the adsorption process for improving the process economics. Regeneration allows for the repeated use of the sorbent material and decreasing costs. After the nine adsorption/desorption cycle, the adsorption capacity of Cd(II) was found to about 82% of the fresh sorbent. The data showed that Cd(II)-imprinted hybrid sorbent had good regeneration capacity for Cd(II).

### CONCLUSION

Cd(II)-imprinted hybrid sorbent sorbent, which was prepared by sol-gel imprinting method, exhibited high adsorption capacity of

Cd(II), a stable uptake of metals at pH in the range of 4-8, fast adsorption kinetics, high selectivity for Cd(II) and facile regeneration property. The kinetic data showed a well fitted pseudo-second-order kinetic model compared to the pseudo-first-order kinetic model, Elovich model and intraparticle diffusion model. The adsorption of Cd(II) on Cd(II)-imprinted hybrid sorbent followed the Redlich-Peterson and Langmuir isotherms with better correlation coefficients. Thermodynamic analysis showed that the adsorption process was endothermic and spontaneous. Organic-inorganic hybrid silica sorbent by combining sol-gel processing and imprinting technique had rich organo-functional groups on the surface of silica and large specific porous framework, ensuring easy, fast and selective adsorption of Cd(II). It was concluded that organic-inorganic hybrid silica imprinted sorbent could be a potential effective sorbent for the selective removal of Cd(II) from aqueous media.

### ACKNOWLEDGEMENTS

The project was sponsored by the program for Liaoning excellent talents in the university of China (grant no. LJQ2011041).

### REFERENCES

1. M. P. Waalkes and S. Rehm, *Fundam. Appl. Toxicol.*, **19**(4), 512 (1992).
2. S. Hydari, H. Shariffard, M. Nabavinia and M. Parvizi, *Chem. Eng. J.*, **193-194**, 276 (2012).
3. K. S. Rao, M. Mohapatra, S. Anand and P. Venkateswarlu, *Int. J. Eng. Sci. Technol.*, **2**(7), 81 (2010).
4. H. Yanagisawa, Y. Matsumoto and M. Machida, *Appl. Surf. Sci.*, **256**(6), 1619 (2010).
5. S. Mustafa, M. Waseem, A. Naeem, K. H. Shah, T. Ahmad and S. Y. Hussain, *Chem. Eng. J.*, **157**(1), 18 (2010).
6. H. M. Baker, *Desalination*, **242**(1-3), 115 (2009).
7. A. M. S. Oancea, M. Radulescu, D. Oancea and E. Pincovschi, *Ind. Eng. Chem. Res.*, **45**(26), 9096 (2006).
8. C. Xiong and C. Yao, *Chem. Eng. J.*, **155**(3), 844 (2009).
9. B. Pan, H. Qiu, B. Pan, G. Nie, L. Xiao, L. Lv, W. Zhang, Q. Zhang and S. Zheng, *Water Res.*, **44**(3), 815 (2010).
10. B. Pan, B. Pan, W. Zhang, L. Lv, Q. Zhang and S. Zheng, *Chem. Eng. J.*, **151**(1-3), 19 (2009).
11. S. Prakash, M. Kumar, B. P. Tripathi and V. K. Shahi, *Chem. Eng. J.*, **162**(1), 28 (2010).
12. J. Aguado, J. M. Arsuaga, A. Arencibia, M. Lindo and V. Gascón, *J. Hazard. Mater.*, **163**(1), 213 (2009).
13. H.-T. Fan, J.-B. Wu, X.-L. Fan, D.-S. Zhang, Z.-J. Su, F. Yan and T. Sun, *Chem. Eng. J.*, **198-199**, 355 (2012).
14. R. Jothiramalingam, S.-L. Lo and L.-A. Phanthei, *Ind. Eng. Chem. Res.*, **49**(6), 2557 (2010).
15. Y. Zhang, W. Liu, L. Zhang, M. Wang and M. Zhao, *Appl. Surf. Sci.*, **257**(23), 9809 (2011).
16. S. Zang and B. Lian, *J. Hazard. Mater.*, **166**(1), 33 (2009).
17. P. X. Sheng, Y.-P. Ting and J. P. Chen, *Ind. Eng. Chem. Res.*, **46**(8), 2438 (2007).
18. N. Candan, N. Tüzmen, M. Andac, C. A. Andac, R. Say and A. Denizli, *Mater. Sci. Eng. C*, **29**(1), 144 (2009).
19. D. K. Singh and S. Mishra, *J. Hazard. Mater.*, **164**(2-3), 1547 (2009).

20. Y. Liu, X. Chang, S. Wang, Y. Guo, B. Din and S. Meng, *Anal. Chim. Acta*, **519**(2), 173 (2004).
21. Z.-C. Li, H.-T. Fan, Y. Zhang, M.-X. Chen, Z.-Y. Yu, X.-Q. Cao and T. Sun, *Chem. Eng. J.*, **171**(7), 703 (2011).
22. M. Gawin, J. Konefał, B. Trzewik, S. Walas, A. Tobiasz, H. Mrowiec and E. Witek, *Talanta*, **80**(3), 1305 (2010).
23. T. P. Rao, R. Kala and S. Daniel, *Anal. Chim. Acta*, **578**(2), 105 (2006).
24. T. P. Rao, S. Daniel and J. M. Gladis, *Trends Anal. Chem.*, **23**(1), 28 (2004).
25. X. Chang, N. Jiang, H. Zheng, Q. He, Z. Hu, Y. Zhai and Y. Cui, *Talanta*, **71**(1), 38 (2007).
26. H.-T. Fan, X. Fan, J. Li, M. Guo, D. Zhang, F. Yan and T. Sun, *Ind. Eng. Chem. Res.*, **51**(14), 5216 (2012).
27. Buhani, Narsito, Nuryono and E. S. Kunarti, *Desalination*, **251**(1-3), 83 (2010).
28. Y.-K. Lu and X.-P. Yan, *Anal. Chem.*, **76**(2), 453 (2004).
29. C. A. Quirarte-Escalante, V. Soto, W. De La Cruz, G. R. Porras, R. Manríquez and S. Gomez-Salazar, *Chem. Mater.*, **21**(8), 1439 (2009).
30. H.-T. Fan, J. Li, Z.-C. Li and T. Sun, *Appl. Surf. Sci.*, **258**(8), 3815 (2012).
31. I. Langmuir, *J. Am. Chem. Soc.*, **40**(9), 1361 (1918).
32. H. M. F. Freundlich, *Z. Phys. Chem.*, **57**, 385 (1906).
33. O. Redlich and D. L. Peterson, *J. Phys. Chem.*, **63**(6), 1024 (1959).
34. S. J. Allen, G. McKay and K. Y. H. Khader, *Environ. Pollut.*, **56**(1), 39 (1989).
35. S. Lagergren, *Kungliga Svenska Vetensk. Handl.*, **24**, 1 (1898).
36. Y. S. Ho and G. McKay, *Process Biochem.*, **34**(5), 451 (1999).
37. M. J. D. Low, *Chem. Rev.*, **60**(3), 267 (1960).
38. W. J. Weber and J. C. Morris, *J. Sanit. Eng. Div. Am. Soc. Civ. Eng.*, **89**, 31 (1963).
39. R. Zhang, B. Wang and H. Ma, *Desalination*, **255**(3), 61 (2010).
40. L. Bois, A. Bonhommé, A. Ribes, B. Pais, G. Raffin and F. Tessier, *Colloids Surf. A*, **221**(1-3), 221 (2003).
41. H.-T. Fan, T. Sun, H.-B. Xu, Y.-J. Yang, Q. Tang and Y. Sun, *Desalination*, **278**(1-3), 238 (2011).